

Modelling of MOF-76(Nd) crystal growth and crystal habit modifications

Ira Amelia¹, Deka Hayuningrum¹, Yahmin Yahmin¹, Meyga Eva Ferama Sari¹, and Nani Farida¹

¹Department of Chemistry, Faculty of Mathematics and Natural Sciences, Universitas Negeri Malang, Jl. Semarang No. 5, Malang 65145, Indonesia

Abstract. MOF-76(Nd) is composed of neodymium(III) ions linked by 1,3,5-benzenetricarboxylate (BTC) ligands to form a 3D polymer framework. MOF-76(Nd) has applications as an adsorbent for Cs(I) and Sr(II) ions in radioactive waste, as well as gas storage and drug nanocarriers. The adsorption capacity of a material depends on its crystal habits. Therefore, modification of MOF-76(Nd) crystal habits by studying and understanding crystal growth is necessary to control its adsorption capacity. However, MOF-76(Nd) crystal growth has not been studied experimentally or theoretically. For that reason, it is crucial to study crystal growth and modify the crystal habits of MOF-76(Nd), which is the purpose of this research, with the limitation of the scope to a theoretical study using *CrystalGrower*. The research focuses on the effects of variations in supersaturation and screw dislocation. Theoretical modification using this software provides an efficient preliminary step before experimental implementation. The simulation results show that supersaturation plays an important role in determining crystal morphology and size. Crystals with an elongated needle-like morphology can be produced under low supersaturation conditions. Meanwhile, crystals with a shorter needle-like morphology can be produced under high supersaturation conditions. In addition, screw dislocation can change the layer-by-layer growth mechanism into a spiral growth mechanism and modify the crystal tips to be blunter. This study provides useful insights into the fundamental aspects of crystal growth and offers a preliminary framework that can guide experimental approaches for achieving desired crystal habits in practical applications.

1 Introduction

Metal Organic Frameworks (MOFs) are composed of inorganic metal ions/metal ion groups and organic ligands (organic linkers) connected by covalent coordination bonds. MOFs have high porosity, large surface area, adjustable pore size, and flexible frameworks. MOFs have various applications, such as catalysts [1], gas separation and storage [2], adsorbents [3] and biomedicine [4]. One MOF, MOF-76(Nd), is composed of neodymium(III) ions connected by 1,3,5-benzenetricarboxylate (BTC) ligands to form a 3D polymer framework [5].

¹ Corresponding author: nfarida@um.ac.id

MOF-76(Nd) demonstrates potential as an adsorbent for Cs(I) and Sr(II) ions in radioactive waste, with an adsorption capacity of 86.20 mg/g for Cs(I) ions and 58.47 mg/g for Sr(II) ions, with a surface area of 582 m²/g [6]. The adsorption capacity level is considered low for an adsorbent. Therefore, modification of the crystal habits of MOF-76(Nd) is necessary to increase its adsorption capacity by increasing the surface area and decreasing the crystal size. To facilitate crystal habit modification, a thorough understanding and study of crystal growth is required. Through comprehensive observation of crystal growth, details during the crystal growth process, such as the role of growth units, solvent ions, structure directing agents, and supersaturation, can be studied.

Crystal growth can be studied experimentally using Atomic Force Microscopy (AFM) to analyze crystal surface topography with high resolution. However, studying crystal growth with AFM is costly. In addition to experimental studies, crystal growth can also be predicted theoretically using *CrystalGrower* software. These predictions can serve as a guide for experimental crystal growth studies with AFM to be more focused. *CrystalGrower* is designed to model crystal growth related to crystal habits and surface topography at the nanoscale using the Monte Carlo method, and can identify crystal defects and screw dislocations in crystals [7]. *CrystalGrower* simulation results provide information related to morphology, estimated crystal size, growth mechanisms, and crystal dissolution [8]–[11]. By understanding the growth mechanism, MOF-76(Nd) crystals can be modified to produce different shapes, morphologies, and sizes by adjusting the synthesis conditions. This data can be used as a prediction to produce MOF-76(Nd) crystals to suit the desired application.

Several MOFs for which crystal growth has been predicted using *CrystalGrower* are HKUST-1, MOF-5, and UiO-66 [7], [8]. The prediction results provide information about the mechanism of growth, morphology, estimated crystal size, supersaturation, and the energy involved. Despite its promising adsorption properties, the crystal growth mechanisms and habit evolution of MOF-76(Nd) remain unexplored, limiting rational morphology control. Therefore, it is necessary to explore the theoretical prediction of crystal growth using *CrystalGrower* and the modification of its crystal habits with variations in supersaturation and screw dislocation.

2 Research Method

2.1 Simulation of MOF-76(Nd) Crystal Growth

To simulate its crystal growth, the MOF-76(Nd) crystallographic data in .CIF file format [12] was simplified into a net file using the *ToposPro* program. The simplification of the file was performed by defining its building units as follows: metal clusters were defined as nodes and organic ligands as linkers. The *ToposPro* converts the nodes into points and the linkers into lines. The output file from *ToposPro* in .TXT format was input into the *CrystalGrower* software to analyze the growth of the MOF-76(Nd) crystal.

In the Simulation Option tab of the *CrystalGrower*, the temperature (T) was set to 80 °C according to the temperature in the experimental MOF-76(Nd) synthesis by Gustafsson *et al.* (2010) [12]. Iterations (I) were set at 5,000,000, and the number of frames was set to 20 for all simulations. The iteration count and number of frames were determined as these numbers are the minimum to give acceptable results. In the Supersaturation Profile tab, the following parameters were input: third-order supersaturation mode, $\Delta\mu_1 = 100$ kcal/mol, $I_1 = 1,000,000$, and $\Delta I_c = 200,000$. The *CrystalGrower* parameters for this simulation were listed in Table 1 (run 1). The interactions between bonds in the MOF-76(Nd) structure were checked in the Net Options tab. Finally, the simulation was executed to generate the output files. These consisted of a visualization file (.vis) and a coordinate file (.xyz), which were subsequently analyzed using the *Ovito* program to observe the crystal surface topography.

2.2 Simulation of MOF-76(Nd) Crystal Habit Modification

The modification of the MOF-76(Nd) crystal habits was performed theoretically using the *CrystalGrower* software. The modification was carried out with supersaturation variations set at $\Delta\mu_1 = 35\text{--}200$ kcal/mol and screw dislocations set in different directions, as shown in Table 1. This supersaturation range was chosen to observe morphological differences from low to high supersaturation. The $\Delta\mu_1 = 35$ kcal/mol was pre-studied as the minimum supersaturation that the MOF-76(Nd) simulation can perform. Additionally, the effect of screw dislocation was used to evaluate its impact on facet thickening and spiral growth mechanisms. It should be noted that this simulation represents a qualitative trend in morphological evolution under ideal conditions, as the model does not explicitly account for solvent effects. The simulation results were read using the *Ovito* visualization program.

Table 1. Variations in crystal growth parameters for crystal habit modification of MOF-76(Nd)

Run	Growth Parameter		
	T (°C)	Supersaturation ($\Delta\mu_1$) (kcal/mol)	Screw Dislocation Direction
1	80	100	-
2	80	35	-
3	80	50	-
4	80	75	-
5	80	125	-
6	80	200	-
7	80	35	[110]
8	80	35	[101]
9	80	35	[001]

3 Results and Discussion

3.1 MOF-76(Nd) Crystal Growth

The MOF-76(Nd) crystal growth simulation for Run 1 results in a needle-like morphology (**Fig. 1**) consistent with the reference [5]. This indicates that the conditions set up in this simulation represent the experimental synthesis conditions from the reference [5]. In this simulation, the supersaturation reached equilibrium at $\Delta\mu_1 = 2.8$ kcal/mol.

The growth mechanism of MOF-76(Nd) crystal is layer-by-layer (**Fig. 1**). The nuclei on the {110} facets create new parallelogram-shaped terraces on the crystal surface, as shown in **Fig. 1(d)**. The parallelogram terraces mimic the crystal's facets' shape, with rapid growth toward the c direction and slow growth toward the a and b directions. A similar phenomenon is observed in DAF-1 and RHO crystal growth, in which the growth rate is faster toward a specific direction to develop the same shape as the crystal's facets [9]. After the nucleus is formed, the growth unit attaches to the step to form a layer of the crystal's facet. The layer will follow the shape of the crystal in accordance with the direction of crystal growth. The growth rate of the nuclei of the MOF-76(Nd) in the [001] direction is larger than that in the [110] direction, resulting in a needle-shaped crystal with pointy tips at each end. This phenomenon is related to the framework structure of MOF-76(Nd) in **Fig. 2**. The growth along the [001] or the c direction

forms Nd–O–Nd chains, which act as the main structural foundation for the structure of MOF-76(Nd)'s 1-dimensional channels. As a comparison, the structures along the [010] and [100] directions are comprised of Nd–BTC–Nd chains, in which a large structure of BTC must be linked between two Nd atoms to grow it. Thus, the growth along the [001] direction is more favourable than that along the [010] and [100] directions. A video of the growth of this crystal can be accessed in the Supporting Information (**Table S1**. Run 1).

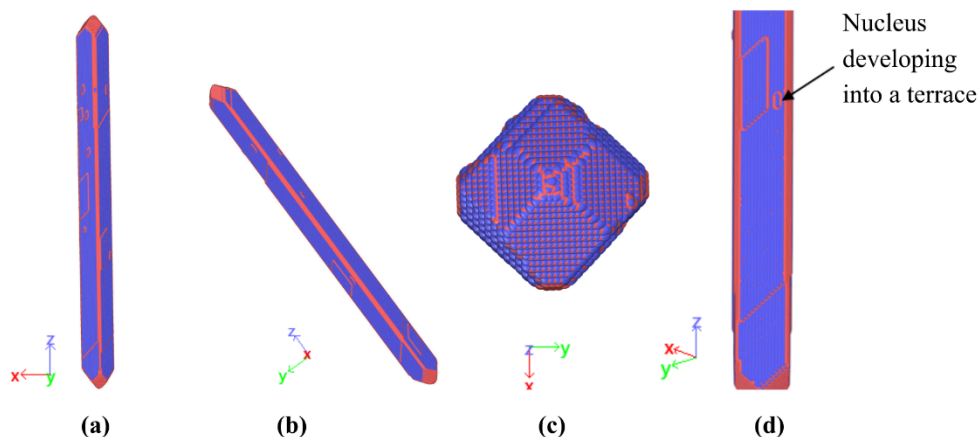


Fig. 1. Simulation of MOF-76(Nd) crystal using *CrystalGrower* with $\Delta\mu_1 = 100$ kcal/mol (**Run 1**).

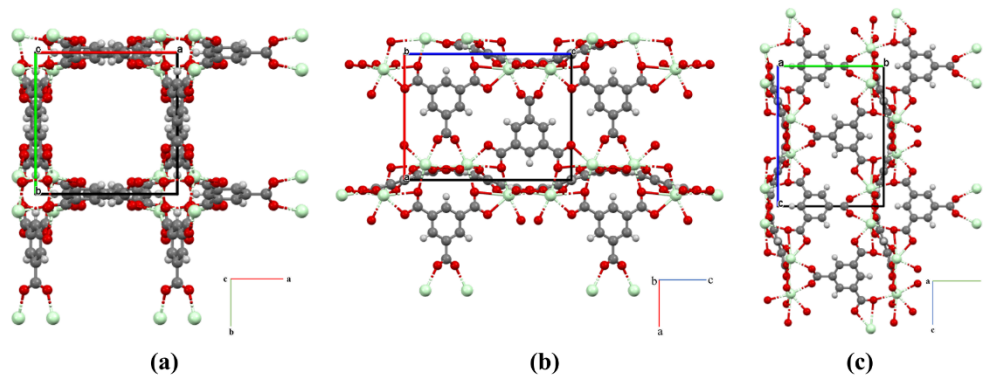


Fig. 2. MOF-76(Nd) structure viewed along (a) [001], (b) [010], and (c) [100] directions. The colours of atoms represent: green = Nd, dark gray = C, light gray = H, and red = O. The box on each structure marks one unit cell.

3.2 MOF-76(Nd) Crystal Habit Modification

3.2.1 Variations of $\Delta\mu_1$

In the *CrystalGrower* simulation, $\Delta\mu_1$ is a parameter that acts as the initial driving force for crystal growth [7]. The higher the value of $\Delta\mu_1$, the greater the supersaturation, leading to a rapid increase in the nucleation rate (crystal core formation). As a result, many small crystals form simultaneously, and their growth becomes irregular. The lower the $\Delta\mu_1$, the lower the

supersaturation, which slows down the nucleation rate and supports more regular crystal growth on existing crystal nuclei, resulting in larger single crystals.

Based on the simulation results, varying the supersaturation to $\Delta\mu_1 = 35 - 75$ kcal/mol (**Fig. 3(a-c)**) produces relatively longer needle-shaped crystals. This may be related to the low initial driving force (nutrient availability), resulting in fewer nuclei. Hence, the nutrients are focused on growing the crystals. As a result, the crystals formed are longer. The controlled growth process results in a layer-by-layer growth mechanism. This has also been explained by Hill *et al.* (2021) [7]. However, since **Run 1** has the lowest supersaturation, the nutrients to grow the crystal are limited, creating the shortest needle among the three simulations (**Fig. 3(a-c)**). More controlled growth at $\Delta\mu_1 = 35$ kcal/mol at **Run 1** leads to very sharp crystal tips compared to those obtained from the other supersaturation values. Meanwhile, increasing the supersaturation to the range of $\Delta\mu_1 = 100 - 200$ kcal/mol (**Fig. 3(d-f)**) produces a shorter needle-shaped crystal morphology. This may be caused by the very high initial driving force, creating a high number of nuclei. Thus, limited nutrients are provided for crystals to grow. This affects the short, needle-shaped crystals, although the growth mechanism remains layer by layer. More detailed images and videos of the simulation with supersaturation variation are provided in the *Supplementary Information* (**Table S1**, Run 1–6).

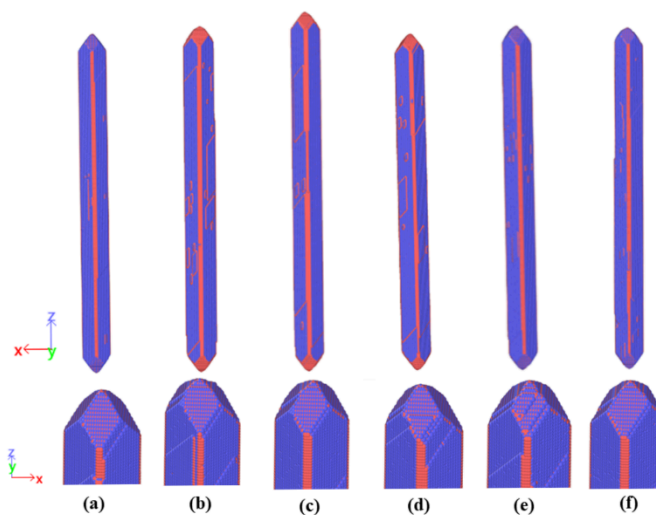


Fig. 3. Predicted MOF-76(Nd) crystal growth with variations of supersaturation at (a) $\Delta\mu_1 = 35$ kcal/mol (**Run 2**), (b) $\Delta\mu_1 = 50$ kcal/mol (**Run 3**), (c) $\Delta\mu_1 = 75$ kcal/mol (**Run 4**), (d) $\Delta\mu_1 = 100$ kcal/mol (**Run 1**), (e) $\Delta\mu_1 = 125$ kcal/mol (**Run 5**), and (f) $\Delta\mu_1 = 200$ kcal/mol (**Run 6**).

In laboratory experiments, supersaturation is related to the concentration of growth “nutrients” (growth units to be added) in the reaction mixture, which is also affected by temperature and pressure. Concentrations may vary depending on how the experiment is conducted, so supersaturation will also vary and affect the crystal growth process and crystal morphology.

3.2.2 Variations of Screw Dislocation

The presence of screw dislocation in crystal growth allows MOF-76(Nd) crystals to grow faster through a spiral growth mechanism (**Fig. 2(a)**). These dislocations create a step on the crystal surface for the attachment of growth units. Crystals with screw dislocations will have a much

faster growth rate toward the screw direction. The crystal growth simulations of the MOF-76(Nd) with a screw dislocation were carried out with $\Delta\mu_1 = 35$ kcal/mol, as this is the lowest supersaturation in this work at which the crystal can start growing.

The addition of screw dislocations can change the layer-by-layer growth mechanism to a spiral one. Ideal crystal growth with a layer-by-layer mechanism is hindered by the high energy required to start a new layer on the crystal surface. The presence of screw dislocations can overcome this by providing a permanent step on the crystal facet for the growth unit to attach to. Crystals with screw dislocations will have a much faster growth rate in the same direction as the screw dislocation. This causes the crystal to thicken on the facet where the screw dislocation is present. With screw dislocations in the $[110]$ direction (**Fig. 4(b)**), the crystal is thicker on the (110) facet, resulting in an asymmetrical needle shape. Without that defect, the growth toward $[110]$ is much slower than that toward $[001]$. The introduction of screw dislocation in the $[101]$ direction (**Fig. 4(c)**) causes the crystal to grow faster on the (101) facet, resulting in a blunt needle-shaped crystal. The introduction of screw dislocation in the $[001]$ direction (**Fig. 4(d)**) causes the crystal to grow faster in the $[001]$ direction, resulting in a blunter needle-shaped crystal. A similar result on SAPO-34-A with a spiral growth was also observed in situ by Smith *et al.* (2025) [13]. More detailed images and videos of the simulation with screw dislocation variation are provided in the *Supplementary Information* (**Table S1**, Run 7–9).

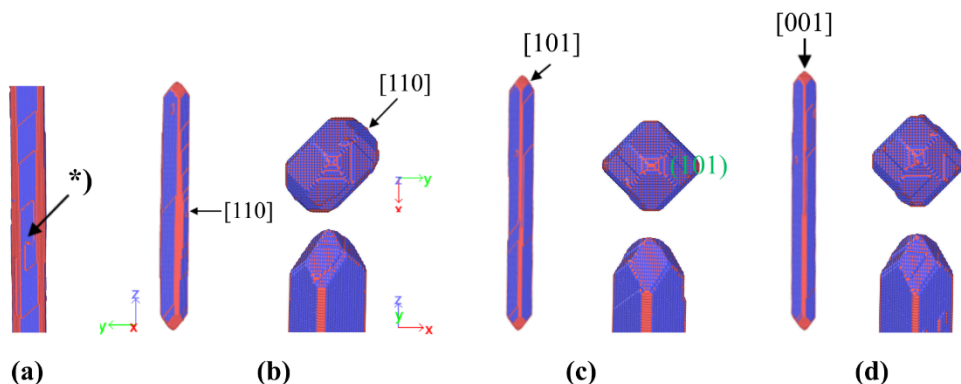


Fig. 4. Modelled MOF-76(Nd) crystal with (a) a screw dislocation on $[110]$ facet (*) as well as its crystal growth modifications with variations of screw dislocation in the direction of (b) $[110]$ (**Run 7**), (c) $[101]$ (**Run 8**), and (d) $[001]$ (**Run 9**). The simulation was set with $\Delta\mu_1 = 35$ kcal/mol.

This study has predicted the ways to modify the crystal habits of MOF-76(Nd). To produce longer crystals, the synthesis could be done with a low-supersaturated synthesis gel to minimise the nuclei formation and maximise the crystal growth toward the $[001]$ direction. The longer the crystals, the lower the surface area, and the longer the 1-dimensional pores. The former condition is unfavourable for adsorption, which requires a high surface area. In contrast, the latter condition could enhance its gas storage application due to the longer 1-dimensional pores, which provide a larger pore volume and make it more effective for storage. However, too long pores will not be beneficial for this purpose because of the pore blocking potential [5].

For drug delivery, MOF-76(Nd) needs to be synthesized at the nanoscale, as this enables efficient cellular uptake of the drug. In addition, a smoother surface is preferable for this purpose [4], meaning that blunt crystals of this MOF are advantageous. Thus, the synthesis conditions are suggested to be set to lead to defects on the crystal tips.

4 Conclusions

This study established a predictive framework for understanding the crystal growth and habit modification of MOF-76(Nd) through *CrystalGrower* simulations. The modeling reveals that the crystal follows a layer-by-layer growth mechanism, with a significantly higher growth rate along the [001] direction than that along the [100] and [010] directions, resulting in an inherently needle-shaped morphology. A key finding of this research is the sensitivity of crystal dimensions to chemical potential; lower supersaturation $\Delta\mu_1 = 35\text{--}75$ kcal/mol promotes elongated structures, whereas higher levels $\Delta\mu_1 = 100\text{--}200$ kcal/mol yield shorter crystals. Furthermore, the introduction of screw dislocations suggests a transition from layer-by-layer to a spiral growth mechanism, leading to localized facet thickening. Based on these theoretical insights, it is hypothesized that increasing the supersaturation of the synthesis gel can effectively limit crystal size by accelerating nucleation rates, thereby enhancing the effective surface area for adsorption. While these findings provide a foundational roadmap for morphology control, further laboratory validation using in situ AFM is urged to empirically verify these growth dynamics and their impact on adsorption performance, as well as their other applications, e.g. as gas storage and drug delivery material.

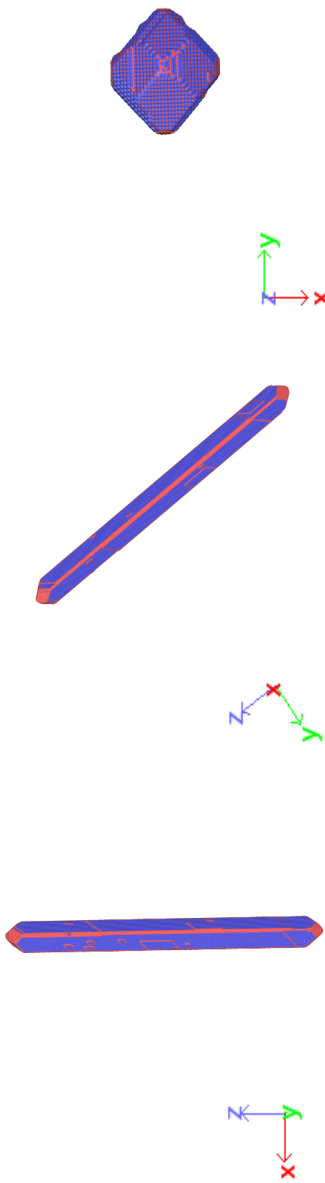
References

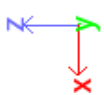

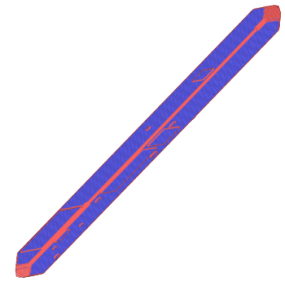

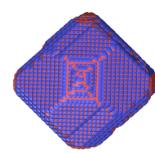
1. X. Sun, Y. Shi, W. Zhang, C. Li, Q. Zhao, J. Gao, and X. Li, "A new type Ni-MOF catalyst with high stability for selective catalytic reduction of NO_x with NH₃," *Catal. Commun.*, vol. **114**, pp. 104–108, (2018)
2. A. Felix Sahayaraj, H. Joy Prabu, J. Maniraj, M. Kannan, M. Bharathi, P. Diwahaar, and J. Salamon, "Metal–Organic Frameworks (MOFs): The Next Generation of Materials for Catalysis, Gas Storage, and Separation," *J. Inorg. Organomet. Polym. Mater.*, vol. **33**, no. 7, pp. 1757–1781, (2023)
3. X. Zhang, J. Maddock, T. M. Nenoff, M. A. Denecke, S. Yang, and M. Schröder, "Adsorption of iodine in metal–organic framework materials," *Chem. Soc. Rev.*, vol. **51**, no. 8, pp. 3243–3262, (2022)
4. Y. Sun, L. Zheng, Y. Yang, X. Qian, T. Fu, X. Li, Z. Yang, H. Yan, C. Cui, and W. Tan, "Metal–Organic Framework Nanocarriers for Drug Delivery in Biomedical Applications," *Nano-Micro Lett.*, vol. **12**, no. 1, p. 103, (2020)
5. A. Garg, M. Almäši, D. Rattan Paul, E. Poonia, J. R. Luthra, and A. Sharma, "Metal-Organic Framework MOF-76(Nd): Synthesis, Characterization, and Study of Hydrogen Storage and Humidity Sensing," *Front. Energy Res.*, vol. **8**, (2021)
6. P. Asgari, S. H. Mousavi, H. Aghayan, H. Ghasemi, and T. Yousefi, "Nd-BTC metal-organic framework (MOF); synthesis, characterization and investigation on its adsorption behavior toward cesium and strontium ions," *Microchem. J.*, vol. **150**, p. 104188, (2019)
7. A. R. Hill, P. Cubillas, J. T. Gebbie-Rayet, M. Trueman, N. de Bruyn, Z. al Harthi, R. J. S. Pooley, M. P. Attfield, V. A. Blatov, D. M. Proserpio, J. D. Gale, D. Akporiaye, B. Arstad, and M. W. Anderson, "CrystalGrower: a generic computer program for Monte Carlo modelling of crystal growth," *Chem. Sci.*, vol. **12**, no. 3, pp. 1126–1146, (2021)
8. M. W. Anderson, J. T. Gebbie-Rayet, A. R. Hill, N. Farida, M. P. Attfield, P. Cubillas, V. A. Blatov, D. M. Proserpio, D. Akporiaye, B. Arstad, and J. D. Gale, "Predicting crystal growth via a unified kinetic three-dimensional partition model," *Nature*, vol. **544**, no. 7651, pp. 456–459, (2017)

9. N. Farida, *Crystal Growth on Complex Framework Structures*. The University of Manchester (United Kingdom), (2019)
10. A. Bachtiar, H. W. Wijaya, I. W. Dasna, and N. Farida, "Study of the ABW-Structured LiZnPO₄ crystallization using X-ray diffraction and CrystalGrower simulation," in *AIP Conference Proceedings*, vol. **2818**, no. 1, (2023)
11. N. Farida, A. W. Ningtyas, E. O. Pertiwi, H. W. Wijaya, D. Danar, and M. E. F. Sari, "Crystal Growth Study of CoZnPO-HEX (CZP) Synthesised using Solvent-Free Method and Its Crystal Growth Simulation," *Akta Kim. Indones.*, vol. **9**, no. 1, pp. 58–69, (2024)
12. M. Gustafsson, A. Bartoszewicz, B. Martín-Matute, J. Sun, J. Grins, T. Zhao, Z. Li, G. Zhu, and X. Zou, "A Family of Highly Stable Lanthanide Metal–Organic Frameworks: Structural Evolution and Catalytic Activity," *Chem. Mater.*, vol. **22**, no. 11, pp. 3316–3322, (2010)
13. R. L. Smith, J. H. Cavka, A. Lind, D. Akporiaye, M. P. Attfield, and M. W. Anderson, "In-Situ Atomic Force Microscopy Study of the Dissolution of Nanoporous SAPO-34 and SAPO-18," *J. Phys. Chem. C*, vol. **119**, no. 49, pp. 27580–27587, (2015)

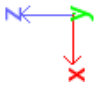
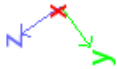
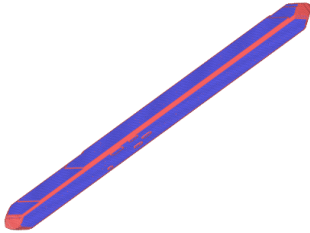
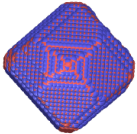
SUPPLEMENTARY DATA**Table S1.** Simulation Results on Modification of MOF-76(Nd) Crystal Habits

<i>Run</i>	<i>T</i> (°C)	<i>Iteration</i>	Growth Parameter		Link
			Supersaturation ($\Delta\mu_1$) (kcal/mol)	Screw Dislocation	
1	80	5,000,000	100	-	https://bit.uconn.edu/~kumard https://bit.uconn.edu/~kumard XPpA4IHK
2	80	5,000,000	35	-	https://bit.uconn.edu/~kumard



<i>Run</i>	T (°C)	Iteration	Growth Parameter		Link
			Supersaturation ($\Delta\mu_1$) (kcal/mol)	Screw Dislocation	
					https://bit.uin.ac.id/n0 KUJ021iQ
	80	5,000,000	75	-	
					https://bit.uin.ac.id/n0 KUJ021iQ
	5,000,000	75	-	-	
					https://bit.uin.ac.id/n0 KUJ021iQ
	75	-	-	-	
					https://bit.uin.ac.id/n0 KUJ021iQ
	5,000,000	-	-	-	
					https://bit.uin.ac.id/n0 KUJ021iQ
	5,000,000	-	-	-	

<i>Run</i>	T (°C)	Iteration	Growth Parameter		Link
			Supersaturation ($\Delta\mu_1$) (kcal/mol)	Screw Dislocation	
5	80	5,000,000	125	-	https://bit.u m.ac.id/qj mksZSVo6

<i>Run</i>	T (°C)	Iteration	Growth Parameter		Link
			Supersaturation ($\Delta\mu_1$) (kcal/mol)	Screw Dislocation	
6	80		5,000,000	-	https://bit.uvyp.ac.id/50j
			200	-	https://bit.uvyp.ac.id/50j
				-	https://bit.uvyp.ac.id/50j
				-	https://bit.uvyp.ac.id/50j

